Biochimie 105 (2014) 84–90

Contents lists available at ScienceDirect

Biochimie

journal homepage: www.elsevier.com/locate/biochi

Research paper

Modeling and molecular dynamics simulations of the V33 variant of the integrin subunit β3: Structural comparison with the L33 (HPA-1a) and P33 (HPA-1b) variants

Vincent Jallu [a, *, 1], Pierre Poulain [b, c, d, e, 1, 2], Patrick F.J. Fuchs [b, c, d, e, 3], Cecile Kaplan [a], Alexandre G. de Brevern [b, c, d, e, **]

[a] Institut National de la Transfusion Sanguine (INTS), Département d'Immunologie Plaquettaire, F-75015 Paris, France
[b] INSERM, U 1134, DSIMB, F-75739 Paris, France
[c] Université Paris Diderot, Sorbonne Paris Cité, UMR_S1134, F-75739 Paris, France
[d] Institut National de la Transfusion Sanguine (INTS), F-75739 Paris, France
[e] Laboratoire d'Excellence GR-Ex, F-75739 Paris, France

ARTICLE INFO

Article history:
Received 7 March 2014
Accepted 21 June 2014
Available online 30 June 2014

Keywords:
Platelet
Integrin alphallb beta3
HPA-1
V33-beta3 antigenicity
Molecular dynamics simulation

ABSTRACT

The human platelet alloantigen (HPA)-1 system, the first cause of alloimmune thrombocytopenia in Caucasians, results from leucine-to-proline substitution (alleles 1a and 1b) of residue 33 in β3 subunit of the integrin αIIbβ3. A third variant with a valine (V33) has been described. Although leucine and valine share similar physicochemical properties, sera containing alloantibodies to the HPA-1a antigen variably reacted with V33-β3, suggesting structural alterations of β3. To analyze the effect of the L33V transition, molecular dynamics simulations were performed on a 3D structural model of the V33 form of the whole β3 extracellular domain (690 residues). Dynamics of the PSI (carrying residue 33), I-EGF-1, and I-EGF-2 domains of β3 were compared to previously obtained dynamics of HPA-1a structure and HPA-1b structural model using classical and innovative developments (a structural alphabet). Clustering approach and local structure analysis showed that L33-β3 and V33-β3 mostly share common structures co-existing in different dynamic equilibria. The L33V substitution mainly displaces the equilibrium between common structures. These observations can explain the variable reactivity of anti-HPA-1a alloantibodies suggesting that molecular dynamic plays a key role in the binding of these alloantibodies. Unlike the L33P substitution, the L33V transition would not affect the structure flexibility of the β3 knee, and consequently the functions of αIIbβ3.

© 2014 Elsevier Masson SAS. All rights reserved.

1. Introduction

The human platelet alloantigen (HPA)-1 system is the first cause of alloimmune thrombocytopenia in Caucasian populations [1,2]. This system is carried by the platelet integrin αIIbβ3 (previously named glycoprotein IIbIIIa) molecule and is characterized by a leucine-to-proline substitution in position 33 of the mature β3 subunit, changing the HPA-1a allele into an HPA-1b allele (NCBI dbSNP accession number rs5918) [3]. The immune response to the HPA-1a allele frequently leads to severe alloimmune thrombocytopenia in incompatible fetuses or neonates and can result in intracranial hemorrhage associated with neurologic sequelae (20% of the cases) or death (10% of the cases). Fetal/neonatal alloimmune thrombocytopenia cases resulting from alloimmunization to HPA-1b are often milder and less frequent. Furthermore, the anti-HPA-1 immune response is complex with several epitopes being

* Corresponding author. INTS, Département d'Immunologie Plaquettaire, 6 rue Alexandre Cabanel, F-75015 Paris, France. Tel.: +33 (0) 1 44 49 30 67; fax: +33 (0) 1 45 67 19 30.
** Corresponding author. INSERM, U1134, DSIMB, Université Paris Diderot, Sorbonne Paris Cité, INTS, 6 rue Alexandre Cabanel, F-75739 Paris, France. Tel.: +33 (0) 1 44 49 30 38; fax: +33 (0) 1 43 06 50 19.
E-mail addresses: vjallu@ints.fr (V. Jallu), alexandre.debrevern@univ-paris-diderot.fr (A.G. de Brevern).
[1] These authors contributed equally to the work.
[2] Present address: Ets Poulain, Pointe-Noire, Congo.
[3] Present address: Dynamique des membranes et trafic intracellulaire, Institut Jacques Monod, CNRS, UMR 7592, Univ. Paris Diderot, Sorbonne Paris Cité, F-75205 Paris, France.

http://dx.doi.org/10.1016/j.biochi.2014.06.017
0300-9084/© 2014 Elsevier Masson SAS. All rights reserved.

recognized by the anti-HPA-1a alloantibodies [4–7]. The HPA-1b allele may also be responsible for an increased risk of thrombosis in patients with cardiovascular diseases [8,9]. Due to its high clinical interest, the HPA-1 system has been largely studied [10].

A V33 allele of β3 resulting from the NM_000212.2:c.175C > G change (no accession number) was identified by Santoso and coworkers [11] during HPA-1 genotyping of a large cohort of patients with thromboembolic disease. These authors also showed that the L33V substitution impairs the reactivity of some alloantibodies directed to the HPA-1a antigen, but not all [11]. However, compared to leucine, valine only lacks a methyl group in its side-chain and both amino acids present similar physicochemical properties [12]. These observations are unexpected and the present study addressed questions about the effect of the L33V substitution on both the structure and the antigenicity of V33-β3.

Crystallographic studies and static molecular models provide important information on the structure–function relationship and disease-related mutations [13,14]. While such models only partially reflect protein structures, molecular dynamics (MD) simulations unveil the flexible nature of proteins necessary to complete various functions and interactions [15,16]. Based on *in silico* modeling and MD simulations, we recently compared the structural dynamics of the HPA-1b form (P33) of β3 with its HPA-1a (L33) form [15].

In this study, using similar *in silico* modeling and MD simulations of the entire extracellular domain of β3, we showed that the L33 and V33 forms of the domains PSI, I-EGF-1 and I-EGF-2 composing the β3 knee mostly share common structures that are in dynamic equilibrium. The L33 to V33 substitution mainly displaces this equilibrium toward structures with locally rigid backbone peptide. This dynamic equilibrium alteration can both explain variable reactivity of anti-HPA-1a alloantibodies and limited structural modifications. Furthermore this study suggests that molecular dynamic plays a key role for high affinity binding of at least some anti-HPA-1a alloantibodies. Unlike proline, valine in position 33 does not affect the global mobility of the domains PSI, I-EGF-1 and I-EGF-2. Consequently functions of the L33-β3 form of αIIbβ3 would not be affected.

2. Materials and methods

2.1. Modeling of V33-β3

An initial L33-β3 structural model was built using a 2.55 Å resolution crystal structure of integrin αIIbβ3 [17] from the Protein Data Bank (PDB) [18] (PDB ID 3FCS) with a homology modeling approach mainly to fill in crystallographic gaps (residues 75–78 and 477–482) and to check for correct assignment of disulfide bonds (see Ref. [15] for more details, model is available in figshare [19]). The L33V substitution was then done using PyMOL software [20]. The final model was composed of 690 residues that correspond to the whole β3 ectodomain. In what follows, the PSI domain of β3 is defined from residue 1 to 56, the I-EGF-1 domain from residue 434 to 472 and the I-EGF-2 domain from residue 473 to 522. According to the supplementary data in Ref. [17], residues 434 and 435 should be assigned to the PSI domain, but for the sake of clarity were assigned to the I-EGF-1 domain here.

2.2. Molecular dynamics simulations, trajectory analyses and Protein Blocks analysis

Five 50 ns MD simulations were performed (using different initial velocities) and one was extended until 100 ns for a total simulation time of 300 ns (simulation protocol is available in figshare [21]). Molecular conformations were saved every 100 ps for further analysis. The first 5 ns of each MD simulation were discarded and trajectory analyses were conducted on a set of two thousand seven hundred forty nine MD snapshots. MD simulations and trajectory analyses were performed as described in Supporting information (Supplementary data S1). Statistical analyses presented here (including trajectory analyses) were restricted to the PSI (residues 1–56), I-EGF-1 (residues 434–472) and I-EGF-2 (residues 473–522) domains. Analysis of Protein Blocks (PBs) [22] gives a reasonable approximation of local protein 3D structures [23]. PBs are a structural alphabet composed of 16 local prototypes, characterized by the φ, ψ dihedral angles description of five consecutive residues. They are labeled from *a* to *p* (see Fig. 1 in Ref. [24]): the PBs *m* and *d* can be roughly described as prototypes for the α-helix and the central β-strand. PBs *a* to *c* primarily represent β-strand N-caps, and PBs *e* and *f*, β-strand C-caps; PBs *g* to *j* are specific to coils, PBs *k* and *l* to α-helix N-caps, and PBs *n* to *p* to α-helix C-caps. PB [25] assignment was carried out using the PBxplore program available on GitHub [26]. The equivalent number of PBs (N_{eq}) [23] is a statistical measurement similar to entropy that represents the average number of PBs a given residue takes. A N_{eq} value of 1 indicates that a single PB is observed, and, at the other extreme, a value of 16 is equivalent to a random distribution. Main structural differences between two proteins were considered significant when at least one of the N_{eq} values was less than 2.5 (N_{eqs} comparison between two residues both with large flexibilities is difficult) and the absolute value of their N_{eq} difference was greater than 1.5.

3. Results

3.1. Structure modeling and molecular dynamics simulation of V33-β3

The V33-β3 structural model was modeled from the L33 form using homology modeling (see Ref. [15] for further details). Considering the PSI, I-EGF-1 and I-EGF-2 domains, after minimization, a root-mean-square deviation (RMSD) value of 1.8 Å calculated on Cα atoms indicated no significant structural modifications between the L33-β3 and V33-β3 models in regards to the size of the proteins.

Five independent MD simulations of the whole β3 ectodomain were performed for a total simulation time of 300 ns for each variant. In each MD simulation, stability of the model was reached after 5 ns and remains stable during the whole simulation times (Fig. S1). Considering the PSI, I-EGF-1 and I-EGF-2 domains, V33-β3 and L33-β3 structural models did not differ with RMSD values of 4.7 ± 0.8 Å and 4.7 ± 0.7 Å respectively; while the RMSD of P33-β3 reaches 7.2 ± 1.0 Å. Fig. 1A shows the difference between the different behaviors. The RMSD profile observed for V33-β3 was mainly unimodal while it was bimodal for L33-β3, indicating that some structural differences exist between the two variants.

To underline the different conformations between the 3 variants, structures obtained from MD simulations were clustered (see Fig. 1B, with clusters ranked according to their frequencies). Nine clusters can be observed, the last five representing are poorly populated (less than 3% for each variant). Two main characteristic clusters dominated: the three variants are largely present in the most populated cluster (e.g. cluster 1), whereas cluster 2 corresponds only to specific P33-β3 conformations never adopted by the two other variants. Cluster 3 reveals specific conformations adopted by P33-β3 and V33-β3 but not by L33-β3, while cluster 4 (and 5) indicates structures common to V33-β3 and L33-β3 but not to P33-β3.

These results suggest that L33-β3 and V33-β3 generally share (95 and 90% of occurrences) similar structural conformations (clusters 1, 4 and 5). In cluster 2, P33-β3 adopted specific

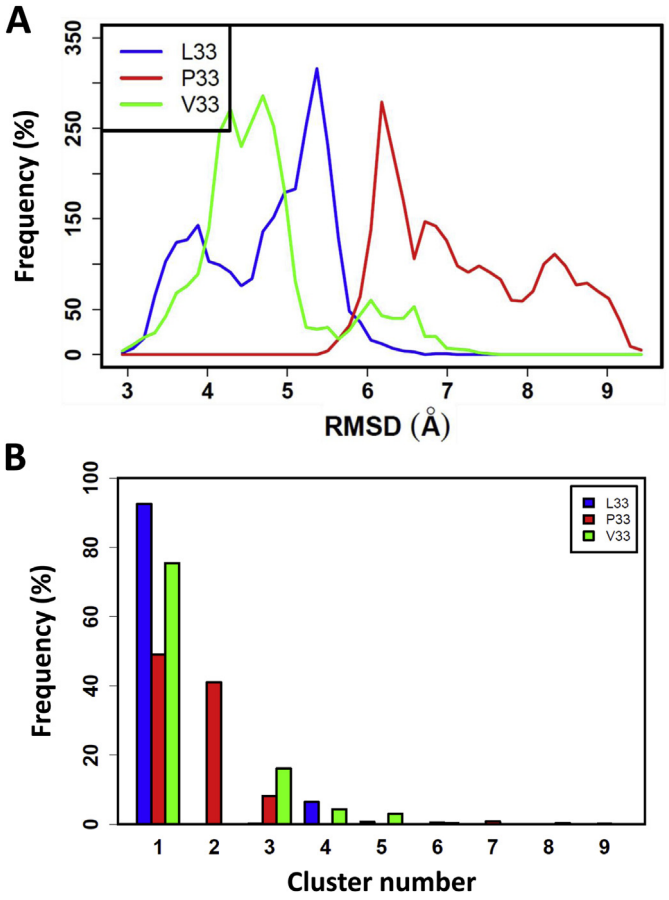

Fig. 1. RMSD and cluster analyses of the PSI, I-EGF-1 and I-EGF-2 domains. (A) RMSD frequencies calculated for Cα atoms from all MD simulations for L33-β3, P33-β3 and V33-β3 are shown (blue, red and green lines, respectively). (B) To compare the behavior of the three β3 forms, a dedicated clustering was performed to highlight their specificities. Structures from MD simulations of the three β3 forms were merged and compared using RMSD computation on the PSI, I-EGF-1 and I-EGF-2 domains. Then, a classical hierarchical clustering approach was performed; it generates clusters of similar overall conformations, i.e. small RMSD values (≤5 Å) within a cluster. Cluster frequencies were then calculated for each β3 form.

conformations (43% of occurrences), but also shared a similar conformation (cluster 3) with V33-β3 in 8% of occurrences. RMSD and clustering analysis suggest that L33-β3 and V33-β3 are mostly structurally similar compared to P33-β3.

Furthermore, as observed for L33-β3 and P33-β3, the root-mean-square fluctuations (RMSF) analysis showed that V33-β3 still presents a high flexibility (up to 6 Å) of the PSI, I-EGF-1 and I-EGF-2 domains (Fig. 2). Nonetheless for RMSF values below 4, this analysis also suggests that some discrete little differences in flexibility do exist, mainly in the PSI domain.

Taken together, these results indicate that the L33V substitution does not significantly affect the structure and the flexibility of the PSI, I-EGF-1 and I-EGF-2 domains contrary to that which was observed in the L33P substitution.

3.2. Local structure equilibrium of the V33-β3 variant

To compare the accessible surface area (ASA) of L, P and V33, a relative ASA (rASA) – ASA normalized to ASA of X in the tri-peptide Ala-X-Ala, X being the considered residue – was calculated (see Supplementary data for more details). The rASA distribution of V33 (mean 63 ± 18%) was similar to that observed for L33 (mean 65 ± 18%), however the peak in frequency (around 60%) suggests

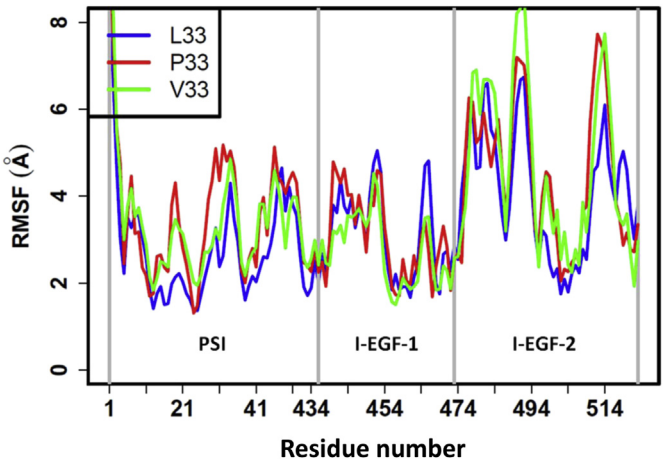

Fig. 2. RMSF of the PSI, I-EGF-1 and I-EGF-2 domains. RMSF values for each residue of the L33 (blue line), the P33 (red line) and the V33 (green line) forms of β3.

that V33 is slightly less exposed than L33 (Fig. 3A). This contrasts with the bimodal distribution observed for the P33 rASA (mean 55 ± 20%) distribution that has a major peak around 40%. Regarding atoms contacts defined by an interatomic distance equal or less than 8 Å (Fig. 3B), V33 (number of contact = 8.2 ± 1.9) showed

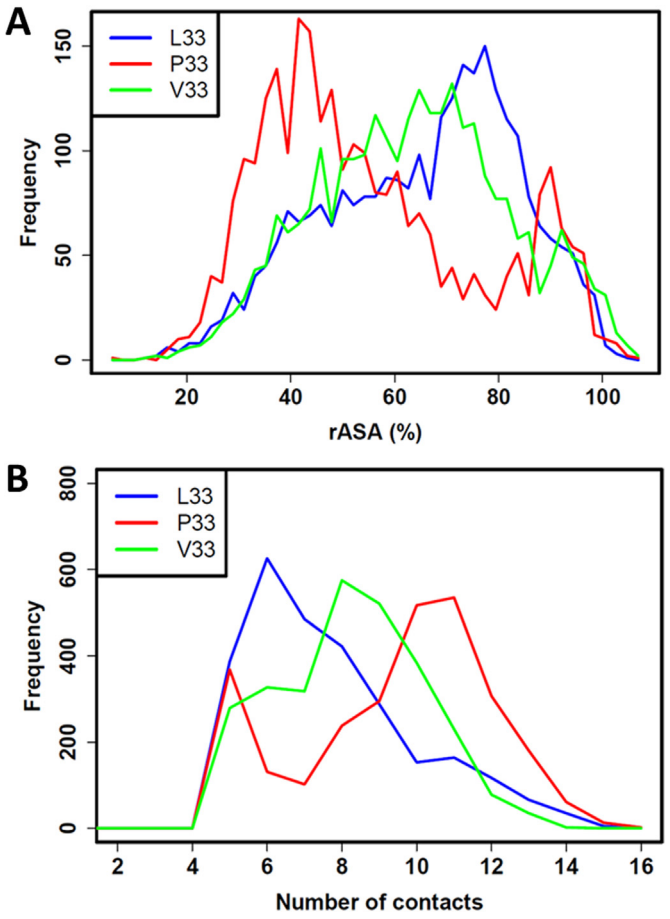

Fig. 3. rASA and number of contacts for L33, P33 and V33. (A) and (B) show the distribution of rASA percentages and the number of contacts, respectively, for L33 (blue), P33 (red) and V33 (green). These distributions show that V33 has a profile intermediate to those of L33 and P33.

behavior intermediate to that of L33 (number of contact = 7.7 ± 2.2) and P33 (number of contact = 9.4 ± 2.5). Regarding details, L33, V33 or P33 residues present similar contact both in number and frequency, with the PSI and the I-EGF-1 domains (Fig. S2 of the Supplementary data). P33 contrasts with L33 and V33 by frequently making high number of contacts with the I-EGF-2 domain (L33 and V33 ≤ 3; P33, up to 8). This reflects the observation that P33 can be frequently buried in the I-EGF-2 domain (see Fig. 5 in Ref. [15]) while it is not the case for L33 and V33.

The distribution of the distances between the center of mass of the residue V33 and the center of mass of the I-EGF-1 showed an unimodal distribution contrasting with the bimodal distribution of L33 and P33 (Fig. 4A). One defining feature of V33 is that its center of mass distances were rarely greater than 15 Å, a distance frequently exceeded in L33 and, to a lesser extent, in P33. Regarding the I-EGF-2 domain (Fig. 4B), the three β3 forms had a common peak around 17–18 Å, but differed in other observed peaks: 1) P33 frequently showed a distance of 10 Å never observed for the two other residues; 2) V33 frequently occupied positions corresponding to a distance around 15 Å never observed for L33; and 3) L33 generally adopted positions corresponding to a distance around 20 Å, less frequently occupied by V33 or P33.

Local structure analysis indicates that the L33V or L33P substitutions displaced the dynamical structure equilibrium of L33-β3 toward new specific equilibria. Nonetheless, the PSI, I-EGF-1 and I-EGF-2 domains of V33-β3 share common characteristics with L33-β3 and in a lesser extent with P33-β3.

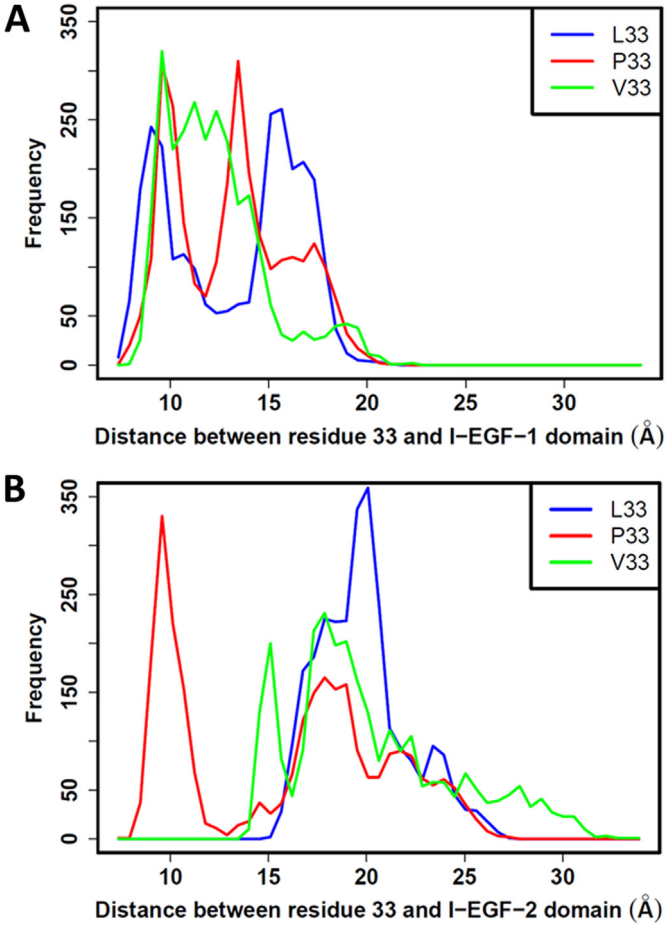

Fig. 4. Distances between residue 33 and I-EGF-1 and I-EGF-2 domains. Center-of-mass distances were measured between L33 (blue line), P33 (red line) or V33 (green line) and the I-EGF-1 (A) or I-EGF-2 (B) domains. For V33, significant differences in distribution were observed regarding both I-EGF-1 and I-EGF-2 domains.

3.3. *Analyses of peptide backbone conformation using the Protein Blocks (PBs) method*

PBs allow to map the 3D structures of a protein into a 1D representation [23]. This method was used to analyze local peptide backbone conformations of the PSI, I-EGF-1, and I-EGF-2 domains induced by the L33V substitution. To statistically assess structure alterations, the equivalent number of PBs or N_{eq} in the three allelic forms were plotted for each residue (see Fig. 5). As observed for L33 and P33, V33 does not affect the high flexibility of the three domains, with most residues adopting more than one PB ($N_{eq} > 1$). Examining the N_{eq} profiles revealed some significant structural alterations characteristic of V33-β3: for residue E29 in the PSI

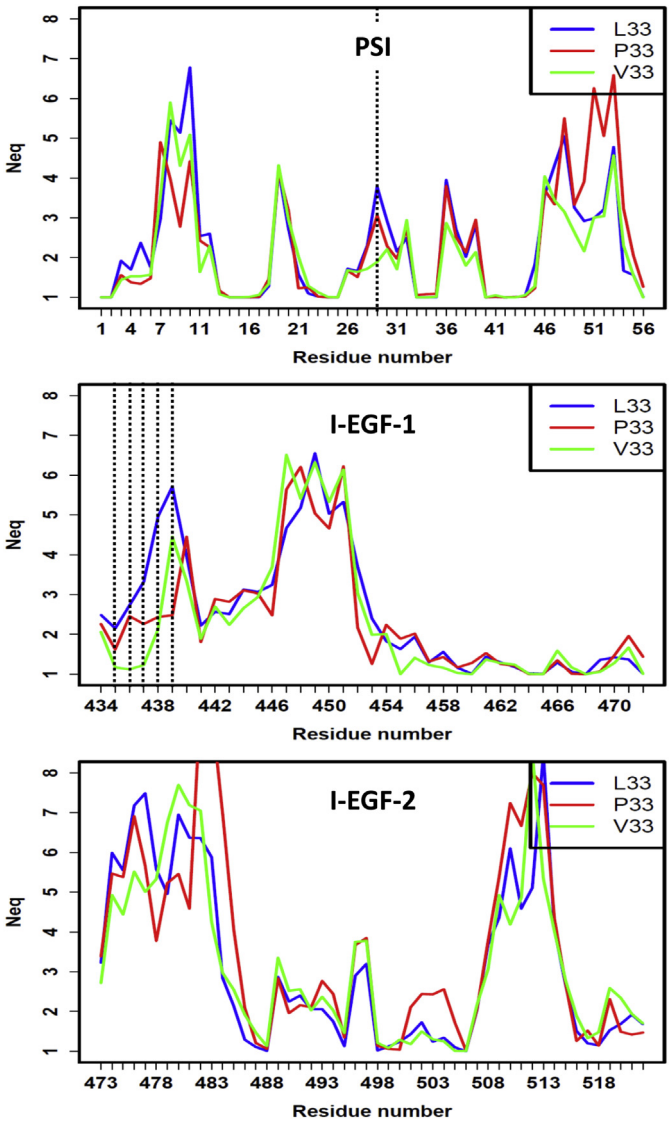

Fig. 5. Local structure and N_{eq} analyses. Shown are N_{eq} values of residues from the PSI, I-EGF-1 and I-EGF-2 domains for L33 (blue line), P33 (red line) and V33 (green line) β3 forms. N_{eq} analyses demonstrated that the three domain structures are highly flexible ($N_{eq} > 1$). In particular, the PSI domain presents four small, interspersed, rigid ($N_{eq} = 1$) areas that are maintained in V33-β3. Residues whose N_{eq} values were differently and significantly affected by the L33P and the L33V substitutions are indicated by vertical dotted lines.

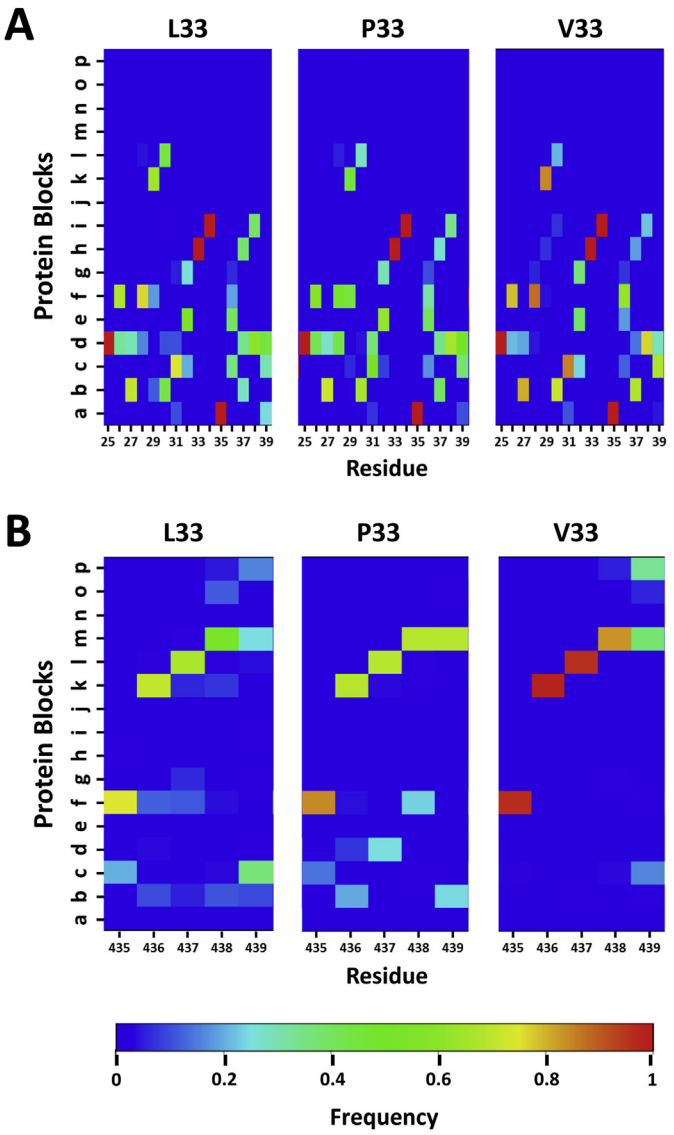

Fig. 6. Protein block analysis of the C26–C38 loop and of the amino acids sequence 435 to 439. These plots show the PBs adopted by each residue of the C26–C38 loop (A) and of the amino-acid sequence 435 to 439 (B) in L33-β3, P33-β3 and V33-β3. A color scale from dark blue (0%) to red (100%) indicates the proportion of each PB adopted by a given residue. The rigid stretch of residues 33–34–35 is maintained in V33-β3, but the L33V substitution stabilizes the PBs adopted by residues 26 to 31. For residues 435 to 437, PBs *f*–*k*–*l* are almost exclusively used in V33-β3, but not in L33-β3 and P33-β3.

domain, the PB *k* is almost exclusively present (>85% of occurrences), whereas in L33-β3 and P33-β3, PB *k* (≈50% of occurrences) but also PBs *b* and *f* (≈20% of occurrences each) are used (Fig. 6A).

Geometrical constraints induce specific successions of PBs [22]. Fig. 6A shows that several PB sequences can characterize the structure encompassing residues 27–31: $_{27}$*bfkbc*$_{31}$, $_{27}$*bdfbc*$_{31}$ and $_{27}$*bdbbc*$_{31}$. Interestingly, the sequence $_{27}$*bfkbc*$_{31}$ is statistically the most dominant structure identified in V33-β3 (90% of occurrences). In L33-β3 and also in P33-β3, other PB sequences are also largely present with about 40% of occurrences like $_{27}$*bdfbc*$_{31}$ or mainly in L33, $_{27}$*bdbbc*$_{31}$. The $_{27}$*bfkbc*$_{31}$ sequence corresponds to a loop strongly maintained by hydrogen bonds while the other two V33-β3 sequences are defined as extended conformations.

Furthermore, in V33-β3, residues $_{435}$CACQ$_{438}$ (I-EGF-1 domain) were mainly associated with the PB sequence $_{435}$*fklm*$_{439}$ (>95% of occurrences, Fig. 6B), which corresponds to a β-turn and starts a helical motif [27]. In L33-β3 and P33-β3, the presence of several less frequent PB sequences (Fig. 6B), specific to extended conformations, reflected a dynamic competition between the dominant and other minor structures. Fig. 7 illustrates these significant structural differences and their frequencies of occurrences respective to L33-β3 and V33-β3.

The four small rigid areas ($N_{eq} = 1$) interspersed with the highly flexible structure ($N_{eq} \geq 2$) of the PSI domain were not affected by the L33V substitution (Fig. 5). The rigid stretch ($N_{eq} = 1$) encompassing residues 33, 34, and 35, which adopted only the PBs sequence *h*, *i* and *a* (Fig. 6A), persists in the presence of a valine in position 33.

PB and N_{eq} analyses showed that the L33V and L33P substitutions differently affect the structure of the PSI, I-EGF-1, and I-EGF-2 domains, but that L33-β3 and V33-β3 share common local structural characteristics in comparison to P33-β3.

4. Discussion

Genotyping a large patient cohort for the HPA-1 system defined by a L33P substitution in β3, allowed identifying a third allele coding for a valine in position 33 of the mature β3 [11]. Some anti-HPA-1a sera can react with V33-β3 while the reactivity of others is partially or fully impaired [11]. The L33V substitution would affect the structure of β3 despite similar physicochemical properties between leucine and valine [12]. To assess these structural modifications, we modeled the V33-β3 variant and performed MD simulations. Structural data of V33-β3 were compared to the previously published results on L33-β3 and P33-β3 [15].

RMSD analyses revealed that the overall structure of the β3 subunit was not affected by the substitution suggesting that L33-β3 and V33-β3 structures generally behave similarly. The intrinsic high flexibility of the β3 knee is conserved. Nonetheless, valine in position 33 does slightly modify the structure of the β3 knee as shown

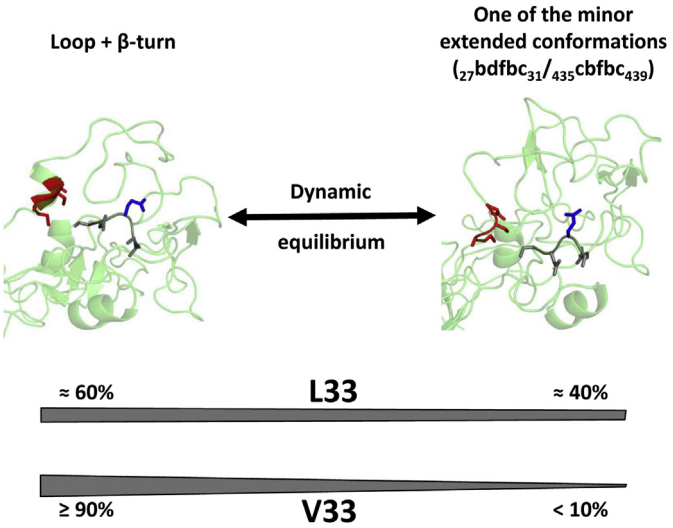

Fig. 7. Most frequent structures in L33-β3 and V33-β3 of residues 27–31 and 435–438. Secondary structures (light green) of the β3 knee of L33 and V33 variants are shown. Worm lines correspond to loops or extended conformations, arrows to β sheets, and ribbons to α-helices or β-turns. Left panel, the dominant structure formed with residues 27–31 (gray) and 435–439 (red) adopting PB sequences $_{27}$*bfkbc*$_{31}$ (loop) and $_{435}$*fklmm*$_{439}$ (β-turn). The side chain of residue E29 is colored in blue. Right panel, one of the minor competing structures adopting extended conformations (shown here PB sequences: $_{27}$*bdfbc*$_{31}$ and $_{435}$*cbfbc*$_{439}$) for L33-β3 and in a lesser extent for V33-β3. The gray double arrows visualize for L33-β3 and V33-β3 the balance (and frequencies) existing between the dominant structure and all minor structures whose only one is shown here (the thickness of the bar is proportional to the frequency).

by specific rASA, contact numbers and distances between the centers of mass. This strikingly differs from P33-β3 where almost all of the structural characteristics studied were significantly modified. In particular, V33 that like L33 has only a few contacts with the I-EGF-2 domains contrasts with P33.

To characterize localization and nature of the structural modifications, PBs analyses carried on the PSI, I-EGF-1 and I-EGF-2 domains were used to compare the three variants for the 3D structure of their peptide backbones. These analyses showed that the β3 knees of L33-β3 and V33-β3 mostly share common structures. Nonetheless from RMSD clustering it can be shown that structures specific of the V33 form of the β3 knee do exist but corresponds to a few number of occurrences. Only P33-β3 presents specific structures with a high frequency (≈40% of occurrences). Interestingly common structures of L33-β3 and V33-β3 are in different dynamical equilibria showing that the main effect of the L33V substitution was to displace this equilibrium. Regarding the structures qualitatively, differences are much localized as observed for the residues stretches 27–31 and 435–438 that respectively belong to the PSI and the I-EGF-1 domains. In both cases, the L33V substitution displace the equilibrium from extended conformations (flexible) toward loop and β-turn tightly maintained by hydrogen bonds (rigid). These structures are highly selected in V33-β3 as shown by a N_{eq} value close to 1 (>90% of occurrences). Although locally rigid these structures do not affect the high intrinsic flexibility of the β3 knee. A previous sequence – structure analysis on a non-redundant protein structure dataset [28] revealed that amino acids with similar physicochemical properties do not necessarily belong to the same 3D structures of the peptide backbone. It was particularly true for leucine and valine. Our study on the L33V substitution in the β3 integrin subunit provides another example.

It has been reported that anti-HPA-1a alloantibodies can bind to different epitopes [4–7]. Our results showed limited structural modifications between V33-β3 and L33-β3, but rather a shift in the dynamical equilibrium of common structures. These observations can underlie the variable reactivity of anti-HPA-1a alloantibodies [11]. A few alloantibodies or monoclonal antibodies have proved to be insensitive to some amino acid replacements [29,30]. Rubinstein et al. suggested that flexibility (of secondary structure elements) in epitopes may facilitate the capacity of epitopes to undergo conformational adjustment upon antibody binding [31]. As L33-β3 and V33-β3 mostly share common structures, the high flexibility of the β3 knee may help compensate for the short side-chain of the valine allowing anti-HPA-1a antibodies reacting with V33-β3. Furthermore because epitopes span 15 to 25 residues [31,32], this suggests that the general topology of some HPA-1a epitope remains unaffected by the L33V substitution.

Two groups of anti-HPA-1a antibodies were defined, depending on their ability to react with the C435A variant of β3 (group I) or not (group II) [5]. Interestingly Santoso et al. [11] reported that the monoclonal antibody CamTram007 from group II failed to react with V33-β3. This observation correlates our results suggesting that the main effect of the L33V substitution results in a structure alteration of the residue stretch 435–438, a region likely affected in the C435A variant of β3 [5] where the disulfide bridge C13–C435 [13] is disrupted. On the other hand, reactivity of monoclonal antibodies 19–7 and 23–15 (group I) remained unaffected [11]. Epitopes of these last antibodies were suspected to locate in the PSI domain [4]. PBs showed that the structure of the PSI domain mostly remained unaffected by the L33V substitution except for residues 27–31. In particular, the structure of the peptide backbone of residues 33–35 is strictly conserved (PBs $_{33}hia_{35}$) whatever the L33, P33 or V33 variant of β3 considered.

MD simulations revealed a highly dynamical nature of the β3 knee and common structures co-exist in different dynamical equilibria that are specific to the considered β3 variant. Dowd et al. [33] showed that some Moabs can neutralize West Nile Viruses as they bind a capsid protein presenting several conformational states in dynamical equilibrium. Although these Moabs bind their epitopes with high affinity, they appear as low affinity antibodies because epitopes are transiently not accessible. A similar hypothesis can be done to explain a loss of affinity for some anti-HPA-1a antibodies reacting to V33-β3 which presents several structures in modified dynamical equilibrium. A second or complementary hypothesis can be proposed. Structural studies combined with kinetic approaches show that antibody isomerization likely occurs during antigen binding [34–36]. The strong structure selectivity observed for residues 27–31 and 435–437 in V33-β3 may thus impair the antibody isomerization that is required for high-affinity binding. This could also explain residual binding or even absence of binding in connection with the variable response of some of the anti-HPA-1a antibodies (sera) that were tested.

Several studies suggest that P33-β3 (HPA-1b) is associated with an increased risk of thrombosis in cardiovascular pathologies [8,9]. Structure modeling and MD simulations of P33-β3 have revealed an increase in flexibility of the β3 knee that can explain increased platelet adhesiveness and possible thrombotic risk [15]. Results of principal component analysis (data not shown) underlined that mobility of the β3 knee (formed by the PSI, I-EGF-1 and I-EGF-2 domains) of V33-β3 and L33-β3 are similar. Furthermore, N_{eq} analysis revealed increased structure selectivity for some residues (27–31 and 435–438) in V33-β3 without affecting flexibility (see RMSF in Fig. 2). Our results indicate that the L33V substitution does not affect the mobility of the β3 knee, suggesting that platelet function is not modified in this variant.

5. Conclusion

To study the structural effects of the L33V substitution, a 3D model of the V33-β3 extracellular domain was obtained using *in silico* mutagenesis of a 3D model of L33-β3 [15]. MD simulations were run and compared with those previously obtained for the L33 (HPA-1a) and P33 (HPA-1b) β3 forms to characterize structural differences. Analyses of MD simulations showed that the L33V substitution does not affect the high intrinsic flexibility of the PSI, I-EGF-1, and I-EGF-2 domains. Specific structures of V33-β3 exist but in only a few occurrences. L33-β3 and V33-β3 mostly share common structures in different dynamical equilibria that are specific of the β3 variant. The main effect of the L33V substitution was to displace the L33-β3 structural equilibrium toward a new equilibrium with a majority of structures locally more rigid. These observations can explain the variable reactivity of anti-HPA-1a alloantibodies suggesting that molecular dynamics play a key role in the binding of these alloantibodies. This study showed that the L33V substitution would not significantly affect the flexibility of the β3 knee, and that αIIbβ3 functions would be unaffected.

Characterization of HPA-1a epitopes is challenging, yet important regarding the high clinical impact of this platelet alloimmune system. A prophylactic treatment for women at risk for anti-HPA-1a alloimmunization by administration of anti-HPA-1a antibodies has been recently proposed [37]. Studies on HPA-1a epitopes are still needed to develop new techniques or applications and to understand underlying mechanisms.

Authorship and disclosures

P.P. and A.G. de B. designed and conducted the experiments; V.J., P.P. and A.G. de B. analyzed the data; V.J. wrote the manuscript; P.F.J.F. and P.P. supervised MD simulation and data analyses; A.G. de

B. and C.K. supervised the research. All authors approved the final manuscript.

Conflict of interest

The authors reported no potential conflicts of interest.

Funding

This work was supported by the French Ministry of Research, Univ. Paris Diderot, Sorbonne Paris Cité, the French National Institute for Blood Transfusion (INTS), the French Institute for Health and Medical Research (INSERM) and "Investissements d'avenir", Laboratories of Excellence GR-Ex. The funders had no role in study design, data collection and analysis, decision to publish, or preparation of the manuscript. The authors were granted access to high performance computing (HPC) resources at the French National Computing Center CINES under grant no. 2012-c2012076723 funded by the GENCI (Grand Equipement National de Calcul Intensif).

Appendix A. Supplementary data

Supplementary data related to this article can be found at http://dx.doi.org/10.1016/j.biochi.2014.06.017.

References

[1] C. Kaplan, J. Freedman, Alloimmune thrombocytopenia, in: A.D. Michelson, Platelets, second ed., 2007, pp. 971–984.
[2] C. Kaplan, Neonatal alloimmune thrombocytopenia, in: K.R. McCrae (Ed.), Thrombocytopenia, 2006, pp. 223–244.
[3] P.J. Newman, R.S. Derbes, R.H. Aster, The human platelet alloantigens, PlA1 and PlA2, are associated with a leucine33/proline33 amino acid polymorphism in membrane glycoprotein IIIa, and are distinguishable by DNA typing, J. Clin. Invest. 83 (1989) 1778–1781.
[4] P. Stafford, C. Ghevaert, K. Campbell, C. Proulx, G. Smith, L.M. Williamson, E. Ranasinghe, N.A. Watkins, J.A. Huntington, W.H. Ouwehand, Immunologic and structural analysis of eight novel domain-deletion beta3 integrin peptides designed for detection of HPA-1 antibodies, J. Thromb. Haemostasis 6 (2008) 366–375. PM:18045240.
[5] N. Valentin, G.P. Visentin, P.J. Newman, Involvement of the cystein-rich domain of glycoprotein IIIa in the expression of the human platelet alloantigen, PI^{A1}: evidence for heterogeneity in the humoral response, Blood 85 (1995) 3028–3033.
[6] L.X. Liu, M. Nardi, J.F. Casella, S. Karpatkin, Inhibition of binding of anti-PlA^1 antibodies to platelets with monoclonal antibody LK-4, evidence for multiple PlA^1 receptor sites on platelet GP IIIa, Blood 88 (1996) 3601–3607.
[7] S. Honda, Y. Honda, B. Bauer, C. Ruan, T.J. Kunicki, The impact of three-dimensional structure on the expression of PI^A alloantigens on human integrin β_3, Blood 86 (1995) 234–242.
[8] D. Burr, H. Doss, G.E. Cooke, P.J. Goldschmidt-Clermont, A meta-analysis of studies on the association of the platelet PlA polymorphism of glycoprotein IIIa and risk of coronary heart disease, Stat. Med. 22 (2003) 1741–1760. PM:12720308.
[9] A. Di Castelnuovo, G. de Gaetano, M.B. Donati, L. Iacoviello, Platelet glycoprotein receptor IIIa polymorphism PLA1/PLA2 and coronary risk: a meta-analysis, Thromb. Haemost. 85 (2001) 626–633. PM:11341496.
[10] R.H. Aster, P.J. Newman, HPA-1a/b(PlA1/A2,Zwa/b): the odyssey of an alloantigen system, Immunohematology 23 (2007) 2–8. PM:17425409.
[11] S. Santoso, H. Kroll, C.L. ndrei-Selmer, I. Socher, A. Rankin, E. Kretzschmar, N.A. Watkins, W.H. Ouwehand, A naturally occurring LeuVal mutation in beta3-integrin impairs the HPA-1a epitope: the third allele of HPA-1, Transfusion 46 (2006) 790–799. PM:16686847.
[12] R.M. Sweet, D. Eisenberg, Correlation of sequence hydrophobicities measures similarity in three-dimensional protein structure, J. Mol. Biol. 171 (1983) 479–488. PM:6663622.
[13] T. Xiao, J. Takagi, B.S. Coller, J.H. Wang, T.A. Springer, Structural basis for allostery in integrins and binding to fibrinogen-mimetic therapeutics, Nature 432 (2004) 59–67. PM:15378069.
[14] V. Jallu, M. Dusseaux, S. Panzer, M.F. Torchet, N. Hezard, J. Goudemand, A.G. de Brevern, C. Kaplan, AlphaIIbbeta3 integrin: new allelic variants in Glanzmann thrombasthenia, effects on ITGA2B and ITGB3 mRNA splicing, expression, and structure-function, Hum. Mutat. 31 (2010) 237–246. PM:20020534.
[15] V. Jallu, P. Poulain, P.F.J. Fuchs, C. plan, A.G. evern, Modeling and molecular dynamics of HPA-1a and -1b polymorphisms : effects on the structure of the β3 subunit of the αIIbβ3 integrin, PLoS One 7 (2012) 1–10.
[16] V. Jallu, G. Bertrand, F. Bianchi, C. Chenet, P. Poulain, C. Kaplan, The alphaIIb p.Leu841Met (Cab3(a+)) polymorphism results in a new human platelet alloantigen involved in neonatal alloimmune thrombocytopenia, Transfusion 53 (2013) 554–563. PM:22738334.
[17] J. Zhu, B.H. Luo, T. Xiao, C. Zhang, N. Nishida, T.A. Springer, Structure of a complete integrin ectodomain in a physiologic resting state and activation and deactivation by applied forces, Mol. Cell 32 (2008) 849–861. PM:19111664.
[18] H.M. Berman, J. Westbrook, Z. Feng, G. Gilliland, T.N. Bhat, H. Weissig, I.N. Shindyalov, P.E. Bourne, The protein data bank, Nucleic Acids Res. 28 (2000) 235–242. PM:10592235.
[19] P. Poulain, A.G. de Brevern, Model of the Beta3 Subunit of Integrin AlphaIIb/beta3, Figshare, 2012. http://dx.doi.org/10.6084/m9.figshare.104602.
[20] W.L. DeLano, The PyMOL Molecular Graphics System, Version 1.5.0.4, Schrödinger, LLC, 2002. http://www.pymol.org.
[21] P. Poulain, A.G. de Brevern, P.F.J. fuchs, Molecular Dynamics Protocol with Gromacs 4.0.7, 2013. http://dx.doi.org/10.6084/m9.figshare.104603.
[22] A.P. Joseph, G. Agarwal, S. Mahajan, J.C. Gelly, L.S. Swapna, B. Offmann, F. Cadet, A. Bornot, M. Tyagi, H. Valadie, B. Schneider, C. Etchebest, N. Srinivasan, A.G. de Brevern, A short survey on protein blocks, Biophys. Rev. 2 (2010) 137–147. PM:21731588.
[23] A.G. de Brevern, C. Etchebest, S. Hazout, Bayesian probabilistic approach for predicting backbone structures in terms of protein blocks, Proteins 41 (2000) 271–287. PM:11025540.
[24] M. Tyagi, A. Bornot, B. Offmann, A.G. de Brevern, Protein short loop prediction in terms of a structural alphabet, Comput. Biol. Chem. 33 (2009) 329–333. PM:19625218.
[25] A.G. de Brevern, New assessment of a structural alphabet, In Silico Biol. 5 (2005) 283–289. PM:15996119.
[26] PBxplore, A Program to Explore Protein Structures with Protein Blocks, 2013. https://github.com/pierrepo/PBxplore.
[27] C. Etchebest, C. Benros, S. Hazout, A.G. de Brevern, A structural alphabet for local protein structures: improved prediction methods, Proteins 59 (2005) 810–827. PM:15822101.
[28] C. Etchebest, C. Benros, A. Bornot, A.C. Camproux, A.G. de Brevern, A reduced amino acid alphabet for understanding and designing protein adaptation to mutation, Eur. Biophys. J. 36 (2007) 1059–1069. PM:17565494.
[29] V. Kosmoliaptsis, T.R. Dafforn, A.N. Chaudhry, D.J. Halsall, J.A. Bradley, C.J. Taylor, High-resolution, three-dimensional modeling of human leukocyte antigen class I structure and surface electrostatic potential reveals the molecular basis for alloantibody binding epitopes, Hum. Immunol. 72 (2011) 1049–1059. PM:21840357.
[30] L.N. Kam-Morgan, S.J. Smith-Gill, M.G. Taylor, L. Zhang, A.C. Wilson, J.F. Kirsch, High-resolution mapping of the HyHEL-10 epitope of chicken lysozyme by site-directed mutagenesis, Proc. Natl. Acad. Sci. U. S. A. 90 (1993) 3958–3962. PM:7683415.
[31] N.D. Rubinstein, I. Mayrose, D. Halperin, D. Yekutieli, J.M. Gershoni, T. Pupko, Computational characterization of B-cell epitopes, Mol. Immunol. 45 (2008) 3477–3489. PM:18023478.
[32] W.G. Laver, G.M. Air, R.G. Webster, S.J. Smith-Gill, Epitopes on protein antigens: misconceptions and realities, Cell 61 (1990) 553–556. PM:1693095.
[33] K.A. Dowd, C.A. Jost, A.P. Durbin, S.S. Whitehead, T.C. Pierson, A dynamic landscape for antibody binding modulates antibody-mediated neutralization of West Nile virus, PLoS Pathog. 7 (2011) e1002111. PM:21738473.
[34] L.C. James, D.S. Tawfik, Structure and kinetics of a transient antibody binding intermediate reveal a kinetic discrimination mechanism in antigen recognition, Proc. Natl. Acad. Sci. U. S. A. 102 (2005) 12730–12735. PM:16129832.
[35] R. Jimenez, G. Salazar, J. Yin, T. Joo, F.E. Romesberg, Protein dynamics and the immunological evolution of molecular recognition, Proc. Natl. Acad. Sci. U. S. A. 101 (2004) 3803–3808. PM:15001706.
[36] Y. Li, H. Li, F. Yang, S.J. Smith-Gill, R.A. Mariuzza, X-ray snapshots of the maturation of an antibody response to a protein antigen, Nat. Struct. Biol. 10 (2003) 482–488. PM:12740607.
[37] J. Kjeldsen-Kragh, H. Ni, B. Skogen, Towards a prophylactic treatment of HPA-related foetal and neonatal alloimmune thrombocytopenia, Curr. Opin. Hematol. 19 (2012) 469–474. PM:22954726.